Present and Future of Rainfall in Antarctica

É. Vignon, M. -L. Roussel, I. V. Gorodetskaya, C. Genthon, A. Berne

Geophysical Research Letters

RESEARCH LETTER
10.1029/2020GL092281

Present and Future of Rainfall in Antarctica

É. Vignon[1,2], M.-L. Roussel[2], I. V. Gorodetskaya[3], C. Genthon[2], and A. Berne[1]

[1]Environmental Remote Sensing Laboratory (LTE), École Polytechnique Fédérale de Lausanne, Lausanne, Switzerland, [2]Laboratoire de Météorologie Dynamique/IPSL/Sorbone Université/CNRS, UMR 8539, Paris, France, [3]Centre for Environmental and Marine Studies (CESAM), Department of Physics, University of Aveiro, Aveiro, Portugal

Key Points:

- First climatological characterization of rainfall occurrence in Antarctica based on meteorological reports and atmospheric reanalyses
- Rain events generally coincide with a warm and moist maritime intrusion and a blocking anticyclone
- CMIP6 scenarios suggest that the overall future warming of Antarctica will be accompanied by more frequent and more intense rainfall events

Supporting Information:

Supporting Information may be found in the online version of this article.

Correspondence to:

É. Vignon,
etienne.vignon@lmd.ipsl.fr

Citation:

Vignon, É., Roussel, M.-L., Gorodetskaya, I. V., Genthon, C., & Berne, A. (2021). Present and future of rainfall in Antarctica. *Geophysical Research Letters*, *48*, e2020GL092281. https://doi.org/10.1029/2020GL092281

Received 23 DEC 2020
Accepted 18 MAR 2021

Abstract While most precipitation in Antarctica falls as snow, little is known about liquid precipitation, although it can have ecological and climatic impacts. This study combines meteorological reports at 10 stations with the ERA5 reanalysis to provide a climatological characterization of rainfall occurrence over Antarctica. Along the East Antarctic coast, liquid precipitation occurs 22 days per year at most and coincides with maritime intrusions and blocking anticyclones. Over the north-western Antarctic Peninsula, rainfall occurs more than 50 days per year on average and the recent summer cooling was accompanied by a decrease of −35 annual rainy days per decade between 1998 and 2015 at Faraday-Vernadsky. Projections from seven latest-generation climate models reveal that Antarctic coasts will experience a warming and more frequent and intense rainfall by the end of the century. Rainfall is expected to impact new regions of the continent, increasing their vulnerability to melting by the preconditioning of surface snow.

Plain Language Summary Given the cold temperatures prevailing across the continent, most precipitation over Antarctica falls as snow. Nonetheless, infrequent rainfall events have already been observed causing serious damage to penguin colonies and facilitating the melting of the snow on the ground surface. Here, we provide the first climatological characterization of rainfall occurrence over Antarctica by examining reports of visual meteorological observations at 10 Antarctic stations. We can evidence the contrast between the coasts of East and West Antarctica that experience a few days per year with liquid precipitation and the western part of the Antarctic Peninsula where rainfall occurs more than 50 days per year on average. The latter region also experienced a significant decrease in rainfall occurrence during the first 15 years of the 21st century. Simulations with latest generation numerical climate models further reveal that the Antarctic continent is projected to undergo an overall warming accompanied by more frequent and more intense rainfall events at the end of century. Rainfall is also expected to impact regions of the continent that currently do not receive rainfall, making them vulnerable to intense events of surface snow melting preceded by liquid precipitation.

1. Introduction

During the austral summer 2013–2014, an Adélie penguin colony near Dumont d'Urville (DDU) station, coastal Adélie Land, Antarctica, experienced a complete reproductive failure, a so-called "zero" year. Among the main reasons for this disaster was an unusual and dramatic rainfall event that occurred on January 1, 2014, and that was responsible for the death of all chicks, whose downy plumage has little waterproofing ability (Ropert-Coudert et al., 2015). According to ice-core records in which water from rainfall and melting manifests as clear frozen layers, two occurrences of heavy liquid precipitation and/or melt could be detected in the decade preceding 2014 in coastal Adélie Land (Goursaud et al., 2017).

At a distance of about 1,500 km to the South-East, the Ross Ice Shelf underwent an extensive, intense, and prolonged surface melt event in January 2016 (Nicolas et al., 2017). Such an event was caused by a strong and sustained advection of warm oceanic air. During the first days of the event, rainfall significantly preconditioned the snowpack by increasing its temperature due to latent heat release from water freezing and hence, contributed to extend the melting. Such a phenomenon has been frequently observed over Greenland (Doyle et al., 2015) but is quite rare in Antarctica.

The phase of Antarctic precipitation can directly impact the surface mass balance of the ice sheet through modulation of the surface albedo (Kirchgäßbner, 2011). Liquid precipitation can also accelerate the retreat

of glaciers by physically eroding the ice or through hydrofracturing when associated with intense surface melting (Pollard et al., 2015). Moreover, non-frozen precipitation falling on frozen surfaces or rocks can directly run off, increasing the fresh water influx into the ocean or into lakes and ponds such as in the Schirmacher Oasis in Queen Maud Land (Kaur et al., 2013). Albeit infrequent, liquid precipitation events can therefore have serious impacts on the fauna and ecosystems, on the climate, and on the mass balance of the Antarctic.

In the Arctic, the largest contribution to the future precipitation increase is predicted to come from rainfall (Bintanja, 2018; Bintanja & Andry, 2017). In the Antarctic, the total precipitation amount over the ice sheet is expected to increase in the coming century (Palerme et al., 2017), but we do not know if and how much the phase of precipitation will change. Overall, very little is known about rainfall occurrence and amount in Antarctica as well as its future evolution.

Our knowledge gap regarding Antarctic rain primarily lies in the technical difficulties in measuring precipitation in the harsh meteorological conditions prevailing on the remote Antarctic continent. Insights might be gained from remotely sensed measurements at stations where radars have been deployed (e.g., Gorodetskaya et al., 2015; Grazioli et al., 2017; Jullien et al., 2020). Preliminary analyses of radar vertical profiles at DDU suggest that during rain events, the melting layer is found in the first hundreds of meters above the ground (Vignon, Besic, et al., 2019). This raises the need for specific high-vertical resolution configurations to detect rainfall from radar observations.

From a satellite perspective, the characterization of rainfall could be possible by means of the W-band cloud profiling radar (CPR) onboard the polar-orbiting CloudSat satellite. The CPR reveals occurrences of "mixed" precipitation over the Antarctic coast, but it does not capture any rainfall events above the ice sheet (Behrangi et al., 2016; Palerme et al., 2014). However, the reliability of those estimations is rather low since (a) the phase of the sampled precipitation is determined by the 2-m temperature predicted by the European Centre for Medium-Range Weather Forecasts (ECMWF) weather analysis and a coarse model of melting layer; (b) CPR data are contaminated by ground-clutter below 1200-m a.g.l., that is, where the melting layer is expected to form at high latitudes; (c) the revisit time of Cloudsat is about 5 days over the coastal margins of the ice sheet (when considering a $1° \times 2°$ grid, Palerme et al., 2014), which questions the ability of the CPR to capture sporadic rainfall events; and (d) over regions with abrupt topography such as the Antarctic Peninsula or the coastal margins, the CPR may receive backscatter from ice surfaces at high altitudes, which can be misinterpreted as being intense near-surface rain rate (Behrangi et al., 2016; Palerme et al., 2019). Other satellite estimations of rainfall occurrences can be obtained from infrared and microwave imager products through the Global Precipitation Climatology Project (GPCP) data set for instance (Adler et al., 2018). However, the determination of the precipitation phase is very indirect since it is based on a look-up table for probability of liquid precipitation as a function of near-surface wet-bulb temperature from atmospheric reanalyses.

Hence, the most reliable information about the Antarctic precipitation phase available so far remains the visual observation by meteorologists that are reported every day at Antarctic stations. Here, we provide the first statistical characterization of rainfall events in Antarctica using a combination of visual meteorological records at 10 Antarctic stations with the ECMWF latest generation atmospheric reanalysis ERA5. Analyzing the recent scenarios from the sixth Coupled Model Intercomparison Project (CMIP6), we further stress that the occurrence and intensity of Antarctic rainfall are expected to significantly increase—and to affect a larger fraction of the continent—during the next century, suggesting that rainfall may be an important meteorological factor to consider for assessing the future of the Antarctic climate and ecosystems.

2. Data and Methods

2.1. Precipitation Observation at 10 Antarctic Stations and Identification of Rainy Days

Visual observations at 10 stations (see Figure 1)—namely DDU, Halley, Neumayer, Rothera, Mawson, Davis, Casey, Syowa, Amundsen-Scott South-Pole, and Vernadsky (ex station Faraday)—have been used to characterize the occurrence of rainfall in Antarctica. These 10 stations have the advantage of (a) being permanent stations so that meteorological observations are therefore available for all seasons, (b) being geographically distributed along the Antarctic periphery (except South Pole) where rainfall is expected to

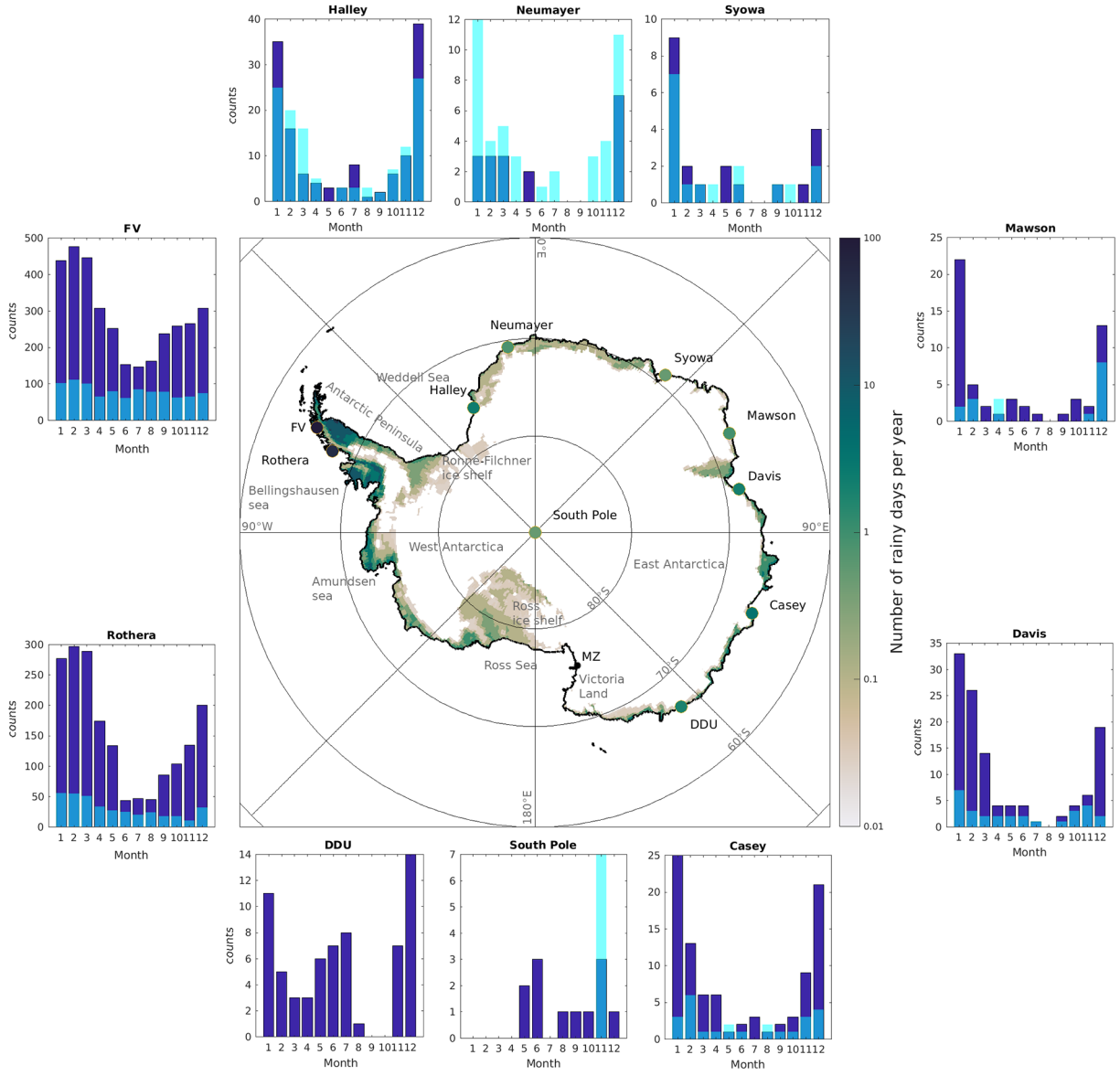

Figure 1. Central panel: Map of the mean annual number of rainy days in the ERA5 reanalysis between 1979 and 2017. Values within circles correspond to the mean annual number of rainy days identified from visual observations at Antarctic stations. Exact numerical values and observation periods for each station are given in Table S1. Days with drizzle are not taken into account in the previous statistics for better consistency with ERA5 which is unable to simulate supercooled drizzle (see supporting information). Note the logarithmic color bar. External panels: Monthly distributions of the number of days with rain (blue) or drizzle (cyan or light-blue when the two overlaps) at 10 Antarctic stations over the respective observation periods (see Table S1). Note that rain-drizzle distinction is not possible from meteorological reports at DDU.

be the most frequent, and (c) containing multi-decadal archives of weather reports that include information on precipitation occurrence and phase at the daily or hourly scale.

At these stations, meteorologists report "present weather"—referring to any weather phenomenon at the time of the observation—and "past weather"—that is, any weather phenomenon that has occurred since the last report—observations. Details on meteorological observations and on the analysis period at each station are given in Section S1. Importantly, it is notable that such observations only allow statements on the occurrence and character of precipitation events, but not on the precipitated amount. Following Turner et al. (2005), we define a rainy day as any day during which there is at least one report of rain or shower in the past or present synoptic weather reports. Days with drizzle are identified with a similar method and we

consider a day with precipitation as any day during which rainfall and/or snowfall is observed. The details on the identification of rainy days at each station are given in Section S1.

2.2. ERA5 Reanalysis

ERA5 is the latest global reanalysis product from the ECMWF (Hersbach et al., 2020). Here, we have used ERA5 data at the standard 0.25° × 0.25° resolution over the 1979–2017 period. ERA5 physics is based on the Cy41r2 version of the Integrated Forecast System. Cloud and large-scale precipitation processes are parameterized with a set of five prognostic equations for the mass mixing ratios of cloud liquid water, cloud ice water, rain, snow, and water vapor (Forbes & Ahlgrimm, 2014; Forbes & Tompkins, 2011). Liquid precipitation is formed by autoconversion and accretion of cloud droplets (Khairoutdinov & Kogan, 2000), or by snowfall melting. Drizzle production through collision-coalescence of supercooled liquid water droplets is not allowed. Forbes et al. (2014) developed a diagnostic algorithm that combines the vertical profiles of temperature, rainfall and snowfall to give the prevailing precipitation type—amongst seven categories—at the surface at a given time. In our study, a day is qualified as "rainy" if the surface precipitation during at least 1 h within the day is classified as either "rain," "freezing rain" or "mixed". As the "mixed" category is somewhat ambiguous, we have verified that our conclusions involving ERA5 still hold when disregarding this category in the identification of rainy days. In Section 3.1, we evaluate the ability of ERA5 to capture Antarctic rain events.

2.3. CMIP6 Global Climate Model Simulations

Future of Antarctic rainfall will be discussed based on the analysis of recent global simulations from seven models—namely IPSL-CM6-LR, CNRM-CM6-1, CanESM5, INM-CM5-0, MIROC6, MRI-ESM2, and GFDL-CM4 - involved in ScenarioMip intercomparison (Eyring et al., 2016; O'Neill et al., 2016) of CMIP6. Details on the cloud and precipitation parameterization in each model are provided in Section S2. We consider two future Shared Socioeconomic Pathways (SSPs) each of them integrating a specific scenario of future climate and societal change (Bauer et al., 2017). The SSP2-4.5 represents the medium part of the range of future forcing pathways and updates the previously used Representative Concentration 4.5 Pathway (RCP 4.5). It envisions a future forcing pathway stabilizing at +4.5 W m^{-2} in which trends continue their historical patterns without substantial deviations. The SSP5-8.5 is an update of the previous RCP 8.5 and assumes an energy intensive, fossil fuel-based economy with a radiative forcing stabilizing at +8.5 W m^{-2}. So-called "Historical" simulations, in which coupled climate models are forced by past atmospheric composition from the middle of the nineteenth century to the early 21st century, have been used to assess models performance. Simulations from the Atmospheric Model Intercomparison Project (AMIP) experiment in which global atmospheric models are forced by observed sea surface temperature and sea ice concentration have been analyzed to assess possible influence of simulated ocean surface conditions by the coupled models. In all models, liquid precipitation is estimated as the difference between total and solid precipitation. Monthly and annual liquid precipitation was calculated for all models, whereas daily amounts could be calculated only for IPSL-CM6A-LR and CNRM-CM6-1.

3. Results

3.1. Antarctic Rainfall at Present

Although visual observations do not allow any quantification of the amount of liquid precipitation, they make possible the characterization of the occurrence of liquid precipitation, namely rain, and drizzle. Figure 1 shows the mean annual number of rainy days from year-round visual observations at 10 stations and from ERA5 that includes diagnostics for the dominant precipitation type. At stations in East and West Antarctica, liquid precipitation occurs between 0 and 4.3 days per year on average over the respective observation periods or 0–3.2 days if considering only rainfall (Table S1). In the north-western sector of the Antarctic Peninsula, Rothera and Faraday/Vernadsky (FV) experience on average 55 and 105 days with liquid precipitation per year (i.e., 22% and 39% of precipitation days), respectively. Although most rainy days occur during the austral summer season—that is, when the temperature during precipitation events is the highest—rain and drizzle also sporadically occur in winter at all stations (Figure 1). Similar conclusions

can be drawn in terms of amount of liquid precipitation in ERA5 for all the Antarctic sectors while the total precipitation rate is generally the lowest in summer (Table S2).

Visual observations reveal that a few liquid precipitation events occurred even at South Pole station between 1992 and 2017 (Table S1). One of the recorded rainy days (24 December 2011) corresponds to the warm intrusion that led to the absolute maximum temperature record at the South Pole on December 25, 2011: −12.3°C (Lazzara et al., 2012). However, provided that cold near-surface temperatures prevail at South Pole (always much below 0°C with an annual mean of −49.5°C, Turner et al., 2020), observations of rain or drizzle at this station very likely correspond to supercooled drizzle events. Given the low concentration of aerosols that can serve as ice nuclei in the Antarctic atmosphere, Silber et al. (2019) show that supercooled liquid drizzle can form and persist at very low temperatures, even below −25°C, in the Ross Ice Shelf sector. The observation of supercooled drizzle at the South Pole and over the Ross Ice Shelf suggests that similar supercooled drizzle events may occur in other regions of the Antarctic continent, even over the high and cold Plateau (especially in summer).

Over the West and East Antarctic margins, ERA5 suggests that rain occurs at most up to 10 days per years and that the annual number of rainy days sharply decreases inland owing to the abrupt temperature gradients imposed by topography and latitude (Figure 1). ERA5 also suggests that rain never occurs in the Ross Sea coast part of Victoria Land along the Transantarctic Mountains. At the Mario Zucchelli (MZ) summer station, this result concurs with the absence of rainfall observation in the meteorological reports (see Section S1.7) and with the study of Scarchilli et al. (2020). The climate of southern Victoria Land is characterized by strong katabatic winds that flow through narrow—and sometimes dry (i.e., ice-free)—valleys down to the coast. The Transantarctic Mountains range together with those strong katabatic winds impede the penetration of warm oceanic air masses to the ice sheet interior (Bromwich, 1989; Turner et al., 2019). The near-surface temperature during precipitation events is therefore too low for snowfall melting to occur (Scarchilli et al., 2020). Occasional rain events nonetheless occur over the northern part of Victoria Land as well as over the Ross Ice Shelf, concurring with the observations of Nicolas et al. (2017) during an extreme melting event in this region.

ERA5 results should, however, be interpreted with caution since the reanalysis shows insufficient performances in capturing rainy days at Antarctic stations. This point is illustrated for four of them with confusion matrices in Figures S1e–S1h. For most stations such as Davis, Halley, and FV, ERA5 underestimates rainfall occurrences. Note that confusion matrices are very similar when considering the nearest fully oceanic model ERA5 grid point instead of the closest grid point (not shown). The rain occurrence underestimation in the reanalysis, therefore, cannot be attributed to differences in altitude between the station and the closest-to-station grid point. It is rather explained by an underestimation of the near-surface temperature (Vignon, Traullé, & Berne, 2019)—that does not exceed 0°C often enough—during precipitation days. This cold bias is noticeable not only at the closest-to-station grid point but also at the nearest fully oceanic model grid point (see red histograms in Figures S1a–S1d). At Casey (Figures S1a and S1e) and Syowa (not shown), ERA5 shows too many rainy days. Such an overestimation compared to visual observations does not necessarily reflect a bias in the reanalysis since meteorologists cannot report all the rain events. Indeed, in cases when rainfall occurs in between observation times or during local night, or when the precipitation rate is very weak, visual observations are less reliable and rainfall occurrences can be missed. Nonetheless, ERA5 was also shown to be overly warm in the coastal Antarctic boundary layer during infrequent but strong heat and moisture transport events when the temperature approaches 0°C (Gorodetskaya, Silva, et al., 2020). This can occasionally induce spurious rain or "mixed-type precipitation" events in the reanalysis.

Rainfall events at most stations correspond to particular synoptic circulation patterns. Along the East Antarctic coast—such as DDU, Syowa, or Neumayer (Figure 2), they coincide with an anticyclonic anomaly (blocking) to the east of the stations (see also Figure S2). Those stations are thereby affected by a pronounced warm and moist maritime intrusion from the north-east sector with strong positive anomalies in tropospheric integrated water vapor (Figure S3) lying within broader regions of warm temperature anomalies (Figure S2). The blocking anticyclone is significantly more intense than during solid precipitation events (Figure 2), which generally correspond to the poleward transit of an extratropical cyclone over the Southern Ocean (Sinclair & Dacre, 2019; Uotila et al., 2011). The Southern Annular Mode (SAM) is the primary mode of climate variability at high southern latitudes whose positive (respectively negative) values

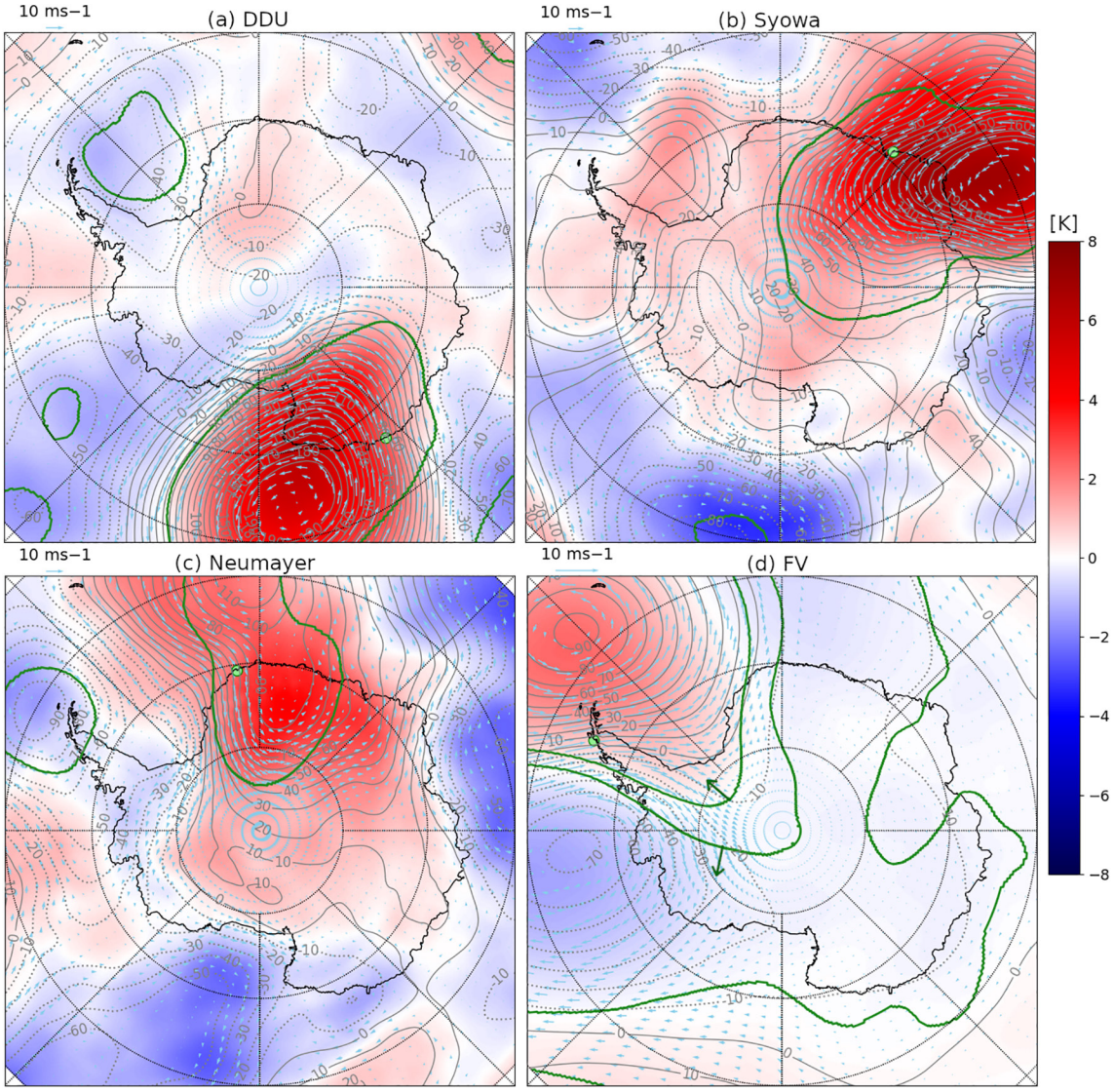

Figure 2. Composite maps of the synoptic circulation from ERA5 during rainy days at four Antarctic stations. Gray contours, color shading, and vectors show the anomaly with respect to the monthly mean of the 500 hPa geopotential height [m], 500 hPa temperature [K], and 500 hPa wind [m s^{-1}], respectively. Dark green outlines show regions where the geopotential height anomaly at each pixel is significantly different from the composite of solid precipitation days (*p*-value from a statistical non-parametric Wilcoxon-Mann-Whitney test ≤1%). Green arrows in panel (d) indicate regions inside contours.

are linked to a stronger (respectively weaker) circumpolar zonal flow above the Southern Ocean and less (respectively more) precipitation over East Antarctica (Genthon et al., 2003; Marshall et al., 2017; Van den Broeke & Van Lipzig, 2004). Negative SAM values generally favor blockings and warm maritime intrusions (Servettaz et al., 2020), explaining why the annual number of rainy days at East Antarctic stations generally negatively correlates with the yearly and summer—when rainfall is the most frequent—SAM indices even though significant correlation is found only for Casey, Mawson, and Syowa (see Table S1). Over the north-western sector of the Antarctic Peninsula, rainfall events are associated with a clear dipole anomaly with a warm ridge to the north-east of the Peninsula's tip and a cold trough over the Bellingshausen sea (Figures 2 and S2) corresponding to strong moist and dry anomalies, respectively (Figure S3). Such a synoptic pattern results in a north-westerly advection of heat and moisture along the western flank of the cyclone toward the Antarctic Peninsula, typically within the warm conveyor belt of the system.

The meteorological report archives also allow us to draw conclusions about the interannual variability of rainfall occurrences at the different stations. When looking at the 1992–2015 period which corresponds to

the longest measurement period common to all stations (except Rothera, see Section S1), Casey and Mawson stations exhibit a moderate but statistically significant (at a 5% level) decrease of −1.74 and −0.83 days per year with rain per decade respectively and of −0.93% and −1.25% of rainy days with respect to the annual number of days with precipitation per decade. A statistically significant increase (at a 5%-level) of +0.38 rainy days per decade is also noticeable at Neumayer station (see Table S1). The most prominent trends are the decrease in the yearly number of days with rain at Rothera (−16.2 days per decade) and FV (−24.2 days per decade). The trend is significant only at a 10% level at Rothera but it is significant at a 1% level at FV even when considering the full measurement period at the station (1979–2015, see Table S1). When looking at the evolution from 1979 to 2015, one can notice that the decrease in the annual number of rainy days at Rothera and FV mostly occurred during the first 15 years of the 21st century. At FV, the decrease reached −35.1 days per decade over the 1998–2015 period (with a 1% level significance) and ERA5 captures it only qualitatively (Figure S4). During the second half of the 20th century, the western sector of the Antarctic Peninsula has been experiencing an increase in precipitation (Lenaerts et al., 2018; Medley & Thomas, 2019; Turner et al., 2005) in response to a significant positive trend in the SAM index in autumn and summer (Marshall, 2003; Marshall et al., 2017) that led to enhanced westerly winds and moisture advections. The surface temperature dramatically increased over the western part of the Antarctic Peninsula (Jones et al., 2019), and particularly at FV (+2.8°C) between 1951 and 1999 (Turner et al., 2005). Consequently, the occurrence of liquid precipitation at FV station also increased during this period as can be seen in Figure S4a for the number of rainy days between 1979 and 2015 and in Figure 3 of Kirchgäßbner (2011) for the number of liquid precipitation events between 1960 and 2000. However, since the end of 1998—beginning of 1999, while the western sector of the Antarctic Peninsula still exhibits an autumn warming (Bozkurt et al., 2020), the Antarctic Peninsula as a whole has been experiencing a marked summer cooling trend (Jones et al., 2019) particularly pronounced in the northern parts (Oliva et al., 2017) owing to the high natural variability of the climate in this region (Turner et al., 2016). Between 1998 and 2015, ERA5 exhibits an overall negative trend of liquid precipitation amount at FV station (−56 mm y^{-1} dec^{-1}), Rothera station (−4.0 mm y^{-1} dec^{-1}) and even at the scale of the whole Antarctic Peninsula (−4.2 mm y^{-1} dec^{-1}, see Table S2). In summer, when rainfall is more frequent, the sea level pressure has been increasing (respectively decreasing) over the Bellingshausen sea (respectively South Atlantic sector) (Turner et al., 2016), disfavoring the circulation pattern associated with liquid precipitation over the north-western part of the Peninsula (Figure 2). Therefore, the regional cooling and the associated synoptic circulation changes during the last two decades may explain the decrease in rainy days at FV and Rothera as well as the pronounced decrease in rainfall amount over the Antarctic Peninsula in ERA5 (Table S2).

Climate models involved in CMIP6 exhibit large differences in their simulation of the total precipitation (Roussel et al., 2020) and of the liquid precipitation amount over Antarctica in the past decades (Figure S6 and Table S3). In particular, the mean amount of liquid precipitation at the continental scale ranges between 0.90 and 10.21 mm y^{-1} between 1979 and 2014 depending on the model. Such differences between models are related to the intrinsic differences in large scale atmospheric circulations and simulated oceanic conditions (Bracegirdle et al., 2015; Krinner et al., 2019), to their horizontal and vertical resolution as well as to their specific subgrid parameterizations of cloud and precipitation (see Section S2). It is worth noting that the dominant precipitation type at each grid cell is not a variable of CMIP6 models' outputs. It is therefore not possible to directly compare rainfall occurrences in CMIP6 simulations with ERA5 without introducing an arbitrary and very sensitive definition of rainy days—based, for instance, on criteria related to liquid precipitation quantity or near-surface temperature—even when we have access to the simulated daily liquid precipitation amount. In terms of liquid precipitation amount estimated as the difference between total precipitation and snowfall from monthly outputs, IPSL-CM6-LR, INM-CM5-0, and MRI-ESM2 are showing quite similar rainfall geographical patterns with respect to the reanalysis despite a lower resolution, with liquid precipitation restricted to coastal areas and the Antarctic Peninsula, particularly the northern part. However, all models but MRI-ESM2 show higher—up to eight times at the continental scale for MIROC6 (see Figures S2 and S3)—rainfall amount compared to ERA5. Nonetheless, one should bear in mind that as ERA5 misses occurrences of rainy days compared to visual observations at most stations, its amount of liquid precipitation in Antarctica may also be underestimated. The true amount is likely in between ERA5 and the CMIP6 models. When prescribing oceanic boundary conditions (so-called AMIP experiments), the overall geographical distribution of rainfall is similar to the Historical simulations for

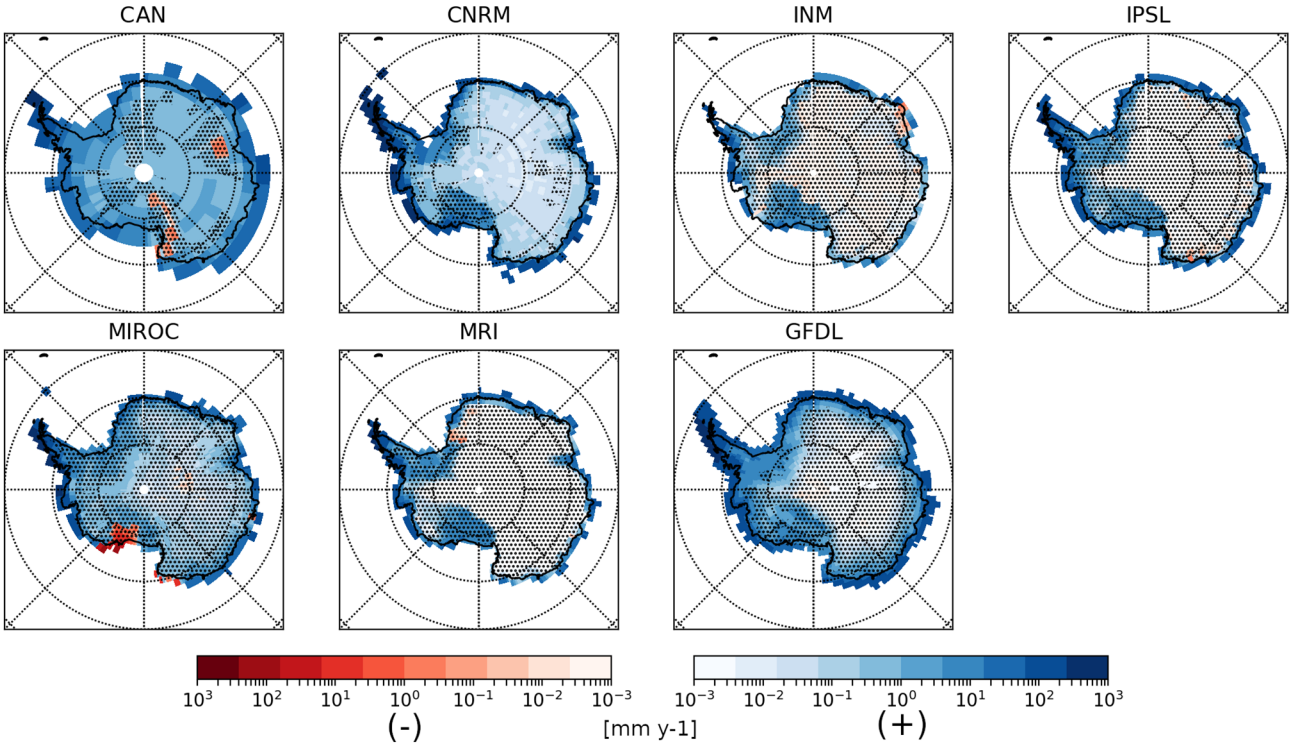

Figure 3. Difference in mean annual liquid precipitation between the 2081–2100 period and the 2015–2034 period in SSP5-8.5 scenarios from seven CMIP6 models. Regions where the difference is not statistically significant—considered here as regions where the 2015–2034 and 2081–2100 liquid precipitation means ± one standard deviation overlap—are shaded with black dots. IPSL, CNRM, CAN, INM, MIROC, MRI, and GFDL acronyms refer to the IPSL-CM6-LR, CNRM-CM6-1, CanESM5, INM-CM5-0, MIROC6, MRI-ESM2, and GFDL-CM4 models, respectively.

each model (Figure S7) but albeit reduced compared to the Historical experiment, significant differences between models persist. The simulated amount of liquid precipitation at the continental scale ranges between 0.67 and 5.65 mm y^{-1} (see Table S4). These large uncertainties regarding the present-day climatology of Antarctic rain from models compel us to be extremely cautious when interpreting the future rain amounts predicted by the CMIP6 scenarios. However, investigating how much more or less liquid precipitation is simulated by a given model in a warming climate, and doing this exercise for all models, permits us to assess the future *relative* evolution of rainfall in Antarctica. In particular, identifying areas where similar and significant trends emerge across models allows us to draw robust conclusions about the vulnerability of some Antarctic regions to future rainfall.

3.2. Future Antarctic Rainfall

Under the high-emissions scenario SSP5-8.5, the seven models analyzed here suggest that Antarctica will experience a warming comprised between 2.5 and 6 K by the end of the century (see Bracegirdle et al., 2020) which will be accompanied by an increase in total precipitation between +27 and +70 mm y^{-1}, consistent with the fact that the saturation vapor pressure air increases with temperature according to the Clausius-Clapeyron relation (Figure S8 and Table S5). Figure 3 shows that models also predict an overall increase in liquid precipitation between the 2081–2100 and 2015–2034 periods. At the continental scale, the averaged liquid precipitation increment equals +7.6 mm y^{-1} (values comprised between +4.6 and +11.3 mm y^{-1}, see Table S5) which corresponds to an averaged relative increase of +240% (relative increments comprised between +74% and +471%). Unlike total precipitation, there is no correlation between the liquid precipitation increase and the surface temperature increment at the continental scale (Figure S8) and similar conclusions hold when conditioning the analysis to different sectors and seasons. As rain events mostly correspond to extreme weather situations and as phase change from snow to rain is a threshold process, this absence of linear correlation is unsurprising.

While the net value of the liquid precipitation increment and its geographical distribution differ between models, all models show an increase in liquid precipitation over almost the entire continent, and a statistically significant increase can be noticed in all simulations over the coastal margins of East Antarctica as well as above the northern and western parts of the Antarctic Peninsula (Figure 3). In addition, the positive trends in liquid precipitation and in liquid precipitation ratio, that is, ratio between liquid precipitation over total precipitation, over the 2015–2100 period are significant at the 1% level for the East Antarctic, West Antarctic, Ross Ice Shelf, Ronne, Filchner Ice Shelves, and Antarctic Peninsula regions in all models (Figure S9 and Table S5). While liquid precipitation corresponds to 0.5%–3.9% of the current total precipitation amount, the increment in liquid precipitation between the 2015–2034 and the 2081–2100 period is expected to explain 15.3% (on average between models; values range in the [8.4%–28.6%] interval) of the increase in total precipitation at the continental scales (Table S5). This value even reaches 56.9% (28.3%–84.1%) when considering the Antarctic Peninsula. Overall, the contribution of liquid precipitation to total precipitation over Antarctica is expected to increase by a factor of 2–5 by the end of the 21st century.

It is worth noting that under an intermediate-emissions scenario (so-called SSP2-4.5), the overall increase in total precipitation is projected to be more limited, but qualitatively similar conclusions regarding the liquid phase can be drawn with a significant positive trend in rainfall during the next century at the continental scale (Figure S10, Table S6) and similar geographical patterns even though some models exhibit local decreases, particularly in West Antarctica (Figure S11).

Examination of the distributions of temperature during precipitation days at particular grid points (corresponding to stations' location) in SSP5-8.5 scenarios from two models (IPSL-CM6A-LR and CNRM-CM6-1) for which we had access to daily outputs of liquid precipitation—shows that the increase in liquid precipitation at the end of the century consistently corresponds to more frequent occurrences of mean daily temperatures above 0°C (Figure S12). Along with the increase in the rain events frequency in the future, the two models also project larger rainfall intensities at all stations (Figure S13). More frequent and more intense rainfall events that generally concur with positive near-surface temperatures may amplify future surface melting events through snowpack preconditioning by water refreezing. In addition to the increase in rainfall frequency and intensity, CMIP6 scenarios also suggest that the areas experiencing days with a mean daily temperature above 0°C and substantial liquid precipitation—so prone to rainfall and snowpack preconditioning and thus enhanced melting (Nicolas et al., 2017)—will expand in the future (Figure 4). The continental areas undergoing more than one day per year with positive temperature and a liquid precipitation amount >1 mm d^{-1} are expected to increase by 1.2×10^6 km^2—that is, by a factor of 2.6— according to the IPSL-CM6A-LR and by 1.8×10^6 km^2—that is, by a factor of 3.3—according to the CNRM-CM6-1 model by the end of the century. The Ronne, Filchner, and Ross Ice Shelves regions are projected to be particularly affected. Sensibly similar conclusions—in terms of geographical distribution—can be drawn from the SSP2-4.5 scenarios (Figure S14). It is thus likely that the vulnerability of the Antarctic margins and main Ice Shelves to rainfall and intense melting events will increase in the next decades, even if the climate follows a trajectory close to an intermediate-emissions scenario.

4. Conclusions

Given the cold temperatures prevailing in Antarctica, most precipitation over the ice sheet falls as snow which accumulates and contributes to its mass balance. Rain events have been frequently reported in the north-western part of the Antarctic Peninsula and more sporadically on the coasts and shelves of East and West Antarctica. Some of these rain events caused serious ecological damages and another important impact of rain over the ice sheet is the snowpack preconditioning to melting. However, little is known about the occurrence and amount of non-frozen precipitation, namely drizzle and rain, over Antarctica. By combining several decades of meteorological reports at 10 Antarctic stations with atmospheric reanalyses, this paper has provided the first climatological characterization of rainfall occurrence in Antarctica. Stations on the East Antarctic coast have reported between 0 and 22 days per year with liquid precipitation that mostly occurs in summer and that generally coincides with a warm intrusion associated with a blocking anticyclone. On the other hand, there is between 50 and 93 rainy days per year on average over the north-western edge of the Antarctic Peninsula. In the latter region, the annual number of rainy days significantly decreased during the summer cooling period at the beginning of the 21st century and the trend reached

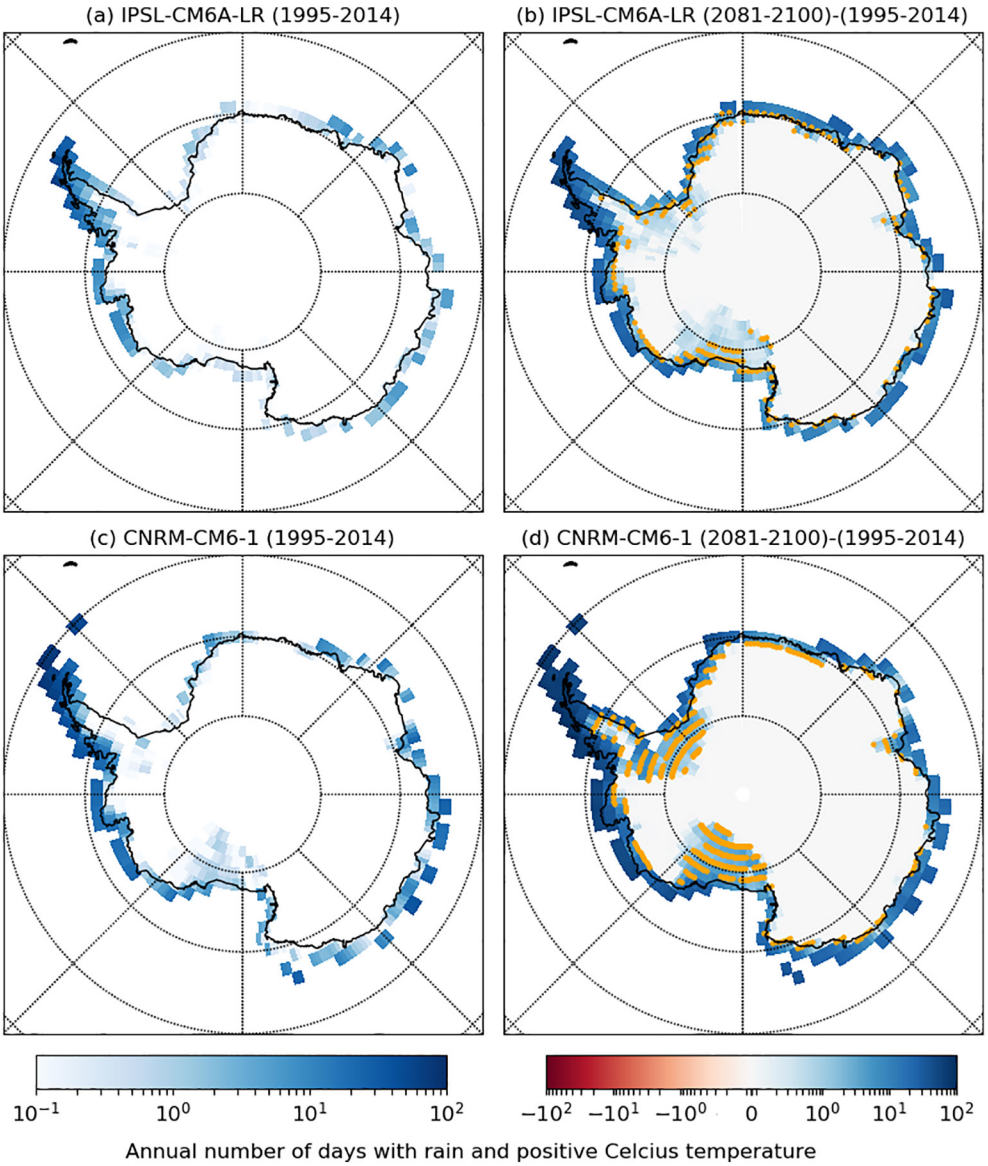

Figure 4. Panels (a and c): Map the annual number of days with substantial rainfall (>1 mm d^{-1}) and temperature >0ºC in historical simulations (1995–2014 period) with the IPSL-CM6A-LR (a) and CNRM-CM6-LR (c) models. Panels (b and d): Corresponding difference between the SSP5-8.5 scenarios (2081–2100 period) and the historical simulation (1995–2014 period). Orange dots indicate pixels where the threshold of 1 day of significant rainfall and temperature >0ºC within a year is exceeded.

−35.1 days per decade over the 1998–2015 period at FV station. The analysis of scenarios from seven state-of-the-art climate models has revealed that the overall future warming of Antarctica will be accompanied by more frequent and more intense rainfall events. In the high-emissions SSP5.85 scenario, the difference in liquid precipitation between the 2081–2100 and 2015–2034 periods equals +7.6 mm y^{-1} on average over the whole Antarctic continent. Liquid precipitation explains on average 15% of the total precipitation increment at the continental scale and almost 57% when considering the region of the Antarctic Peninsula. A deeper analysis of projection using the IPSL-CM6A-LR and CNRM-CM6-1 models suggests that continental areas that can experience temperatures greater than 0°C together with significant liquid precipitation amount will increase by a factor of about 3 by the end of the century, expanding particularly over the Ronne, Filchner, and Ross Ice Shelves. Those regions will therefore be exposed to a higher risk of melting by the preconditioning of surface snow. However, there is a large difference in the liquid precipitation amount predicted

by the different CMIP6 models. Given the expected increasing importance of rainfall for the Antarctic climate, those differences call for further attention to the evaluation and improvement of the representation of precipitation microphysics and phase in climate models over Antarctica.

Data Availability Statement

Data from Mario Zucchelli station were obtained with the help of Claudio Scarchilli. This research project was fostered and initiated in the framework of the APRES3 program (http://apres3.osug.fr/) with the support of the French Polar Institute (IPEV).

Acknowledgments
The authors thank Météo France, and in particular, Olivier Traullé and Pascal Herrera for providing access to the in situ measurements and observations at Dumont d'Urville. The Japan meteorological agency, the Alfred Wegener Institute, the British Antarctic Survey, the Australian Bureau of Meteorology, the Antarctic Meteorological Research Center (AMRC), Automatic Weather Station (AWS) programs, and the National Antarctic Scientific Center of Ukraine are gratefully acknowledged for maintaining and distributing meteorological observations in Antarctica. Irina Gorodetskaya thanks FCT/MCTES for the financial support to CESAM (UIDP/50017/2020+UIDB/50017/2020) and project ATLACE (CIRCNA/CAC/0273/2019) through national funds. The authors thank two anonymous reviewers for their careful evaluation of the manuscript and thoughtful comments as well as Monika Feldmann for her help with English editing.

References

Adler, R., Sapiano, M., Huffman, G., Wang, J.-J., Gu, G., Bolvin, D., et al. (2018). The global precipitation climatology project (GPCP) monthly analysis (new version 2.3) and a review of 2017 global precipitation. *Atmosphere*, *9*(4), 138. https://doi.org/10.3390/atmos9040138

Bauer, N., Calvin, K., Emmerling, J., Fricko, O., Fujimori, S., Hilaire, J., et al. (2017). Shared socio-economic pathways of the energy sector – Quantifying the narratives. *Global Environmental Change*, *42*, 316–330. https://doi.org/10.1016/j.gloenvcha.2016.07.006

Behrangi, A., Christensen, M., Richardson, M., Lebsock, M., Stephens, G., Huffman, G. F., et al. (2016). Status of high-latitude precipitation estimates from observations and reanalyses. *Journal of Geophysical Research: Atmospheres*, *121*(9), 4468–4486. https://doi.org/10.1002/2015JD024546

Bintanja, R. (2018). The impact of arctic warming on increased rainfall. *Scientific Reports*, *8*(1), 1–6. https://doi.org/10.1038/s41598-018-34450-3

Bintanja, R., & Andry, O. (2017). Towards a rain-dominated arctic. *Nature Climate Change*, *7*(4), 263–267. https://doi.org/10.1038/nclimate3240

Bozkurt, D., Bromwich, D. H., Carrasco, J., Hines, K. M., Maureira, J. C., & Rondanelli, R. (2020). Recent near-surface temperature trends in the Antarctic Peninsula from observed, reanalysis and regional climate model data. *Advances in Atmospheric Sciences*, *37*, 477–493. https://doi.org/10.1007/s00376-020-9183-x

Bracegirdle, T. J., Krinner, G., Tonelli, M., Haumann, F. A., Naughten, K. A., Rackow, T., et al. (2020). Twenty first century changes in antarctic and southern ocean surface climate in CMIP6. *Atmospheric Science Letters*, *21*, e984. https://doi.org/10.1002/asl.984

Bracegirdle, T. J., Stephenson, D. B., Turner, J., & Phillips, T. (2015). The importance of sea ice area biases in 21st century multimodel projections of antarctic temperature and precipitation. *Geophysical Research Letters*, *42*(24), 10832–10839. https://doi.org/10.1002/2015GL067055

Bromwich, D. H. (1989). An extraordinary katabatic wind regime at Terra Nova Bay, Antarctica. *Monthly Weather Review*, *117*(3), 688–695. https://doi.org/10.1175/1520-0493(1989)117⟨0688:AEKWRA⟩2.0.CO;2

Doyle, S. H., Hubbard, A., Van De Wal, R. S. W., Box, J. E., Van As, D., Scharrer, K., et al. (2015). Amplified melt and flow of the Greenland ice sheet driven by late-summer cyclonic rainfall. *Nature Geoscience*, *8*(8), 647–653. https://doi.org/10.1038/ngeo2482

Eyring, V., Bony, S., Meehl, G. A., Senior, C. A., Stevens, B., Stouffer, R. J., & Taylor, K. E. (2016). Overview of the coupled model intercomparison project phase 6 (CMIP6) experimental design and organization. *Geoscientific Model Development*, *9*(5), 1937–1958. https://doi.org/10.5194/gmd-9-1937-2016

Forbes, R. M., & Ahlgrimm, M. (2014). On the representation of high-latitude boundary layer mixed-phase cloud in the ECMWF global model. *Monthly Weather Review*, *142*, 3425–3445. https://doi.org/10.1175/mwr-d-13-00325.1

Forbes, R., & Tompkins, A. (2011). An improved representation of cloud and precipitation. *ECMWF Newsletter*, *129*, 13–18.

Forbes, R., Tsonevsky, I., Hewson, T., & Leutbecher, M. (2014). Toward predicting high-impact freezing rain events. *ECMWF Newsletter*, *41*, 15–21.

Genthon, C., Krinner, G., & Sacchettini, M. (2003). Interannual Antarctic tropospheric circulation and precipitation variability. *Climate Dynamics*, *21*, 289–307. https://doi.org/10.1007/s00382-003-0329-1

Gorodetskaya, I. V., Kneifel, S., Maahn, M., Van Tricht, K., Thiery, W., Schween, J. H., et al. (2015). Cloud and precipitation properties from ground-based remote-sensing instruments in east Antarctica. *The Cryosphere*, *9*(1), 285–304. https://doi.org/10.5194/tc-9-285-2015

Gorodetskaya, I. V., Silva, T., Schmithüsen, H., & Hirasawa, N. (2020). Atmospheric River signatures in radiosonde profiles and reanalyses at the Dronning Maud Land Coast, East Antarctica. *Advances in Atmospheric Sciences*, *37*(5), 455–476. https://doi.org/10.1007/s00376-020-9221-8

Goursaud, S., Masson-Delmotte, V., Favier, V., Preunkert, S., Fily, M., Gallée, H., et al. (2017). A 60-year ice-core record of regional climate from Adélie Land, coastal Antarctica. *The Cryosphere*, *11*(1), 343–362. https://doi.org/10.5194/tc-11-343-2017

Grazioli, J., Genthon, C., Boudevillain, B., Duran-Alarcon, C., Del Guasta, M., Madeleine, J.-B., & Berne, A. (2017). Measurements of precipitation in Dumont d'Urville, Adélie Land, East Antarctica. *The Cryosphere*, *11*, 1797–1811. https://doi.org/10.5194/tc-11-1797-2017

Hersbach, H., Bell, B., Berrisford, P., Hirahara, S., Horányi, A., Muñoz-Sabater, J., et al. (2020). The ERA5 global reanalysis. *Quarterly Journal of the Royal Meteorological Society*, *146*, 1999–2049. https://doi.org/10.1002/qj.3803

Jones, M. E., Bromwich, D. H., Nicolas, J. P., Carrasco, J., Plavcová, E., Zou, X., & Wang, S.-H. (2019). Sixty years of widespread warming in the southern middle and high latitudes (1957-2016). *Journal of Climate*, *32*(20), 6875–6898. https://doi.org/10.1175/JCLI-D-18-0565.1

Jullien, N., Vignon, É., Sprenger, M., Aemisegger, F., & Berne, A. (2020). Synoptic conditions and atmospheric moisture pathways associated with virga and precipitation over coastal Adélie Land in Antarctica. *The Cryosphere*, *14*(5), 1685–1702. https://doi.org/10.5194/tc-14-1685-2020

Kaur, R., Dutta, H. N., Deb, N. C., Gajananda, K., Srivastav, M. K., & Lagun, V. E. (2013). Investigation of unusual atmospheric warming over the Schirmacher oasis, East Antarctica. *International Journal of Science and Technology*, *2*(7).

Khairoutdinov, M., & Kogan, Y. (2000). A new cloud physics parameterization in a large-eddy simulation model of marine stratocumulus. *Monthly Weather Review*, *128*(1), 229–243. https://doi.org/10.1175/1520-0493(2000)128⟨0229:ANCPPI⟩2.0.CO;2

Kirchgäßbner, A. (2011). An analysis of precipitation data from the antarctic base Faraday/Vernadsky. *International Journal of Climatology*, *31*(3), 404–414. https://doi.org/10.1002/joc.2083

Krinner, G., Beaumet, J., Favier, V., Déqué, M., & Brutel-Vuilmet, C. (2019). Empirical run-time bias correction for antarctic regional climate projections with a stretched-grid AGCM. *Journal of Advances in Modeling Earth Systems*, *11*(1), 64–82. https://doi.org/10.1029/2018MS001438

Lazzara, M. A., Keller, L. M., Markle, T., & Gallagher, J. (2012). Fifty-year Amundsen-Scott South Pole station surface climatology. *Atmospheric Research*, *118*, 240–259. https://doi.org/10.1016/j.atmosres.2012.06.027

Lenaerts, J. T., Fyke, J., & Medley, B. (2018). The signature of ozone depletion in recent antarctic precipitation change: A study with the community earth system model. *Geophysical Research Letters*, *45*(23), 12–931. https://doi.org/10.1029/2018gl078608

Marshall, G. J. (2003). Trends in the southern annular mode from observations and reanalyses. *Journal of Climate*, *16*(24), 4134–4143. https://doi.org/10.1175/1520-0442(2003)016⟨4134:TITSAM⟩2.0.CO;2

Marshall, G. J., Thompson, D. W. J., & Broeke, M. R. (2017). The signature of Southern Hemisphere atmospheric circulation patterns in Antarctic precipitation. *Geophysical Research Letters*, *44*, 580–611. https://doi.org/10.1002/2017GL075998

Medley, B., & Thomas, E. R. (2019). Increased snowfall over the antarctic ice sheet mitigated twentieth-century sea-level rise. *Nature Climate Change*, *9*(1), 34–39. https://doi.org/10.1038/s41558-018-0356-x

Nicolas, J. P., Vogelmann, A. M., Scott, R. C., Wilson, A. B., Cadeddu, M. P., Bromwich, D. H., et al. (2017). January 2016 extensive summer melt in West Antarctica favored by strong El Niño. *Nature Communications*, *8*, 15799. https://doi.org/10.1038/ncomms15799

Oliva, M., Navarro, F., Hrbáček, F., Hernández, A., Nývlt, D., Pereira, P., et al. (2017). Recent regional climate cooling on the Antarctic Peninsula and associated impacts on the cryosphere. *The Science of the Total Environment*, *580*, 210–223. https://doi.org/10.1016/j.scitotenv.2016.12.030

O'Neill, B. C., Tebaldi, C., van Vuuren, D. P., Eyring, V., Friedlingstein, P., Hurtt, G., et al. (2016). The Scenario Model Intercomparison Project (ScenarioMIP) for CMIP6. *Geoscientific Model Development*, *9*(9), 3461–3482. https://doi.org/10.5194/gmd-9-3461-2016

Palerme, C., Claud, C., Wood, N. B., L'Ecuyer, T., & Genthon, C. (2019). How does ground clutter affect CloudSat snowfall retrievals over ice sheets? *IEEE Geoscience and Remote Sensing Letters*, *16*(3), 342–346. https://doi.org/10.1109/lgrs.2018.2875007

Palerme, C., Genthon, C., Claud, C., Kay, J. E., Wood, N. B., & L'Ecuyer, T. (2017). Evaluation of current and projected antarctic precipitation in CMIP5 models. *Climate Dynamics*, *48*(1), 225–239. https://doi.org/10.1007/s00382-016-3071-1

Palerme, C., Kay, J. E., Genthon, C., L'Ecuyer, T., Wood, N. B., & Claud, C. (2014). How much snow falls on the Antarctic ice sheet? *The Cryosphere*, *8*, 1577–1587. https://doi.org/10.5194/tc-8-1577-2014

Pollard, D., DeConto, R. M., & Alley, R. B. (2015). Potential Antarctic Ice Sheet retreat driven by hydrofracturing and ice cliff failure. *Earth and Planetary Science Letters*, *412*, 112–121. https://doi.org/10.1016/j.epsl.2014.12.035

Ropert-Coudert, Y., Kato, A., Meyer, X., Pellé, M., MacIntosh, A. J. J., Angelier, F., et al. (2015). A complete breeding failure in an Adélie penguin colony correlates with unusual and extreme environmental events. *Ecography*, *38*(2), 111–113. https://doi.org/10.1111/ecog.01182

Roussel, M.-L., Lemonnier, F., Genthon, C., & Krinner, G. (2020). Brief communication: Evaluating antarctic precipitation in ERA5 and CMIP6 against CloudSat observations. *The Cryosphere*, *14*(8), 2715–2727. https://doi.org/10.5194/tc-14-2715-2020

Scarchilli, C., Ciardini, V., Grigioni, P., Iaccarino, A., De Silvestri, L., Proposito, M., et al. (2020). Characterization of snowfall estimated by in situ and ground-based remote-sensing observations at Terra Nova Bay, Victoria Land, Antarctica. *Journal of Glaciology*, *66*(260), 1006–1023. https://doi.org/10.1017/jog.2020.70

Servettaz, A. P. M., Orsi, A. J., Curran, M. A. J., Moy, A. D., Landais, A., Agosta, C., et al. (2020). Snowfall and water stable isotope variability in East Antarctica controlled by warm synoptic events. *Journal of Geophysical Research - D: Atmospheres*, *125*, e2020JD032863. https://doi.org/10.1029/2020JD032863

Silber, I., Fridlind, A. M., Verlinde, J., Ackerman, A. S., Chen, Y. S., Bromwich, D. H., et al. (2019). Persistent supercooled drizzle at temperatures below −25°C observed at McMurdo Station, Antarctica. *Journal of Geophysical Research - D: Atmospheres*, *124*(20), 10878–10895. https://doi.org/10.1029/2019JD030882

Sinclair, V. A., & Dacre, H. F. (2019). Which extratropical cyclones contribute most to the transport of moisture in the Southern Hemisphere? *Journal of Geophysical Research - D: Atmospheres*, *124*(5), 2525–2545. https://doi.org/10.1029/2018JD028766

Turner, J., Lachlan-Cope, T., Colwell, S., & Marshall, G. J. (2005). A positive trend in western antarctic peninsula precipitation over the last 50 years reflecting regional and antarctic-wide atmospheric circulation changes. *Annals of Glaciology*, *41*, 85–91. https://doi.org/10.3189/172756405781813177

Turner, J., Lu, H., White, I., King, J. C., Phillips, T., Hosking, J. S., et al. (2016). Absence of 21st century warming on Antarctic Peninsula consistent with natural variability. *Nature*, *535*, 411–415. https://doi.org/10.1038/nature18645)

Turner, J., Marshall, G. J., Clem, K., Colwell, S., Phillips, T., & Lu, H. (2020). Antarctic temperature variability and change from station data. *International Journal of Climatology*, *40*(6), 2986–3007. https://doi.org/10.1002/joc.6378

Turner, J., Phillips, T., Thamban, M., Rahaman, W., Marshall, G. J., Wille, J. D., et al. (2019). The dominant role of extreme precipitation events in antarctic snowfall variability. *Geophysical Research Letters*, *46*(6), 3502–3511. https://doi.org/10.1029/2018GL081517

Uotila, P., Vihma, T., Pezza, A. B., Simmonds, I., Keay, K., & Lynch, A. H. (2011). Relationships between antarctic cyclones and surface conditions as derived from high-resolution numerical weather prediction data. *Journal of Geophysical Research*, *116*(D7). https://doi.org/10.1029/2010JD015358

Van den Broeke, M., & Van Lipzig, N. (2004). Changes in antarctic temperature, wind and precipitation in response to the antarctic oscillation. *Annals of Glaciology*, *39*, 19–27. https://doi.org/10.3189/172756404781814654

Vignon, É., Besic, N., Jullien, N., Gehring, J., & Berne, A. (2019). Microphysics of snowfall over coastal east antarctica simulated by polar WRF and observed by radar. *Journal of Geophysical Research - D: Atmospheres*, *124*(21), 11452–11476. https://doi.org/10.1029/2019JD031028

Vignon, É., Traullé, O., & Berne, A. (2019). On the fine vertical structure of the low troposphere over the coastal margins of East Antarctica. *Atmospheric Chemistry and Physics*, *19*(7), 4659–4683. https://doi.org/10.5194/acp-19-4659-2019

References From the Supporting Information

Boucher, O., Servonnat, J., Albright, A. L., Aumont, O., Balkanski, Y., Bastrikov, V., et al. (2020). Presentation and evaluation of the IPSL-CM6A-LR climate model. *Journal of Advances in Modeling Earth Systems*, *12*(7), e2019MS002010. https://doi.org/10.1029/2019MS002010

Hajima, T., Watanabe, M., Yamamoto, A., Tatebe, H., Noguchi, M. A., Abe, M., et al. (2020). Development of the MICRO-ES21 earth system model and the evaluation of biogeochemical processes and feedbacks. *Geoscientific Model Development*, *13*(5), 2197–2244. https://doi.org/10.5194/gmd-13-2197-2020

Hourdin, F., Rio, C., Grandpeix, J.-Y., Madeleine, J.-B., Cheruy, F., Rochetin, N., et al. (2020). LMDZ6A: The atmospheric component of the IPSL climate model with improved and better tuned physics. *Journal of Advances in Modeling Earth Systems. 12*(7), e2019MS001892. https://doi.org/10.1029/2019MS001892

Kawai, H., Yukimoto, S., Koshiro, T., Oshima, N., Tanaka, T., Yoshimura, H., & Nagasawa, R. (2019). Significant improvement of cloud representation in the global climate model MRI-ESM2. *Geoscientific Model Development*, *12*(7), 2875–2897. https://doi.org/10.5194/gmd-12-2875-2019

Lohmann, U., & Roeckner, E. (1996). Design and performance of a new cloud microphysics scheme developed for the ECHAM general circulation model. *Climate Dynamics*, *12*(8), 557–572.

Lopez, P. (2002). Implementation and validation of a new prognostic large-scale cloud and precipitation scheme for climate and data-assimilation purposes. *Quarterly Journal of the Royal Meteorological Society*, *128*(579), 229–257. https://doi.org/10.1256/00359000260498879

Madeleine, J.-B., Hourdin, F., Grandpeix, J.-Y., Rio, C., Dufresne, J.-L., Konsta, D., et al. (2020). Improved representation of clouds in the LMDZ6A global climate model. *Journal of Advances in Modeling Earth Systems*, *12*. https://doi.org/10.1029/2020MS002046

Rimbu, N., Lohmann, G., König-Langlo, G., Necula, C., & Ionita, M. (2012). 30 years of synoptic observations from Neumayer Station with links to datasets [data set]. In *Daily to intraseasonal oscillations at Antarctic research station Neumayer. Antarctic Science* (Vol. *26*, pp. 193–204). https://doi.org/10.1017/S0954102013000540

Roehrig, R., Beau, I., Saint-Martin, D., Alias, A., Decharme, B., Guérémy, J.-F., et al. (2020). The CNRM global atmosphere model ARPEGE-Climat 6.3: Description and evaluation. *Journal of Advances in Modeling Earth Systems*, *12*(7), e2020MS002075. https://doi.org/10.1029/2020MS002075

Rotstayn, L. D. (1997). A physically based scheme for the treatment of stratiform clouds and precipitation in large-scale models. I: Description and evaluation of the microphysical processes. *Quarterly Journal of the Royal Meteorological Society*. *123*(541), 1227–1282. https://doi.org/10.1002/qj.49712354106

Swart, N. C., Cole, J. N. S., Kharin, V. V., Lazare, M., Scinocca, J. F., Gillett, N. P., et al. (2019). The Canadian Earth System Model version 5 (CanESM5.0.3). *Geoscientific Model Development*, *12*(11), 4823–4873. https://doi.org/10.5194/gmd-12-4823-2019

Tatebe, H., Ogura, T., Nitta, T., Komuro, Y., Ogochi, K., Takemura, T., et al. (2019). Description and basic evaluation of simulated mean state, internal variability, and climate sensitivity in MICRO6. *Geoscientific Model Development*, *12*(7), 2727–2765. https://doi.org/10.5194/gmd-12-2727-2019

Tiedtke, M. (1993). Representation of clouds in large-scale models. *Monthly Weather Review*, *121*(11), 3040–3061.

Voldoire, A., Saint-Martin, D., Sénési, S., Decharme, B., Alias, A., Chevallier, M., et al. (2019). Evaluation of CMIP6 deck experiments with CNRM-C-6-1. *Journal of Advances in Modeling Earth Systems*, *11*(7), 2177–2213. https://doi.org/10.1029/2019MS001683

Volodin, E., Mortikov, E., Kostrykin, S., Galin, V. Y., Lykossov, V., Gritsun, A., et al. (2017). Simulation of the present-day climate with the climate model INMCM5. *Climate Dynamics*, *49*(11–12), 3715–3734.

Volodin, E. M., Mortikov, E. V., Kostrykin, S. V., Galin, V. Y., Lykossov, V. N., Gritsun, A. S., et al. (2018). Simulation of the modern climate using the INM-CM48 climate model. *Russian Journal of Numerical Analysis and Mathematical Modelling*, *33*(6), 367–374.

Watanabe, S., Hajima, T., Sudo, K., Nagashima, T., Takemura, T., Okajima, H., et al. (2011). MICRO-ESM 2010: Model description and basic results of CMIP5-20c3m experiments. *Geoscientific Model Development*, *4*(4), 845–872. https://doi.org/10.5194/gmd-4-845-2011

Zhao, M., Golaz, J.-C., Held, I. M., Guo, H., Balaji, V., Benson, R., et al. (2018). The GFDL global atmosphere and land model AM4.0/LM4.0: 1. Simulation characteristics with prescribed SSTs. *Journal of Advances in Modeling Earth Systems*, *10*(3), 691–734. https://doi.org/10.1002/2017MS001208